

Supplemental Figure S1

Figure S1. Sequences of VDAC mutants.

Sequence alignment of VDAC34, VDAC36 and the 21 mutants. VDAC34 sequence was used as reference and amino acids differing on the other protein sequences are indicated in grey background.

Supplemental Figure S2

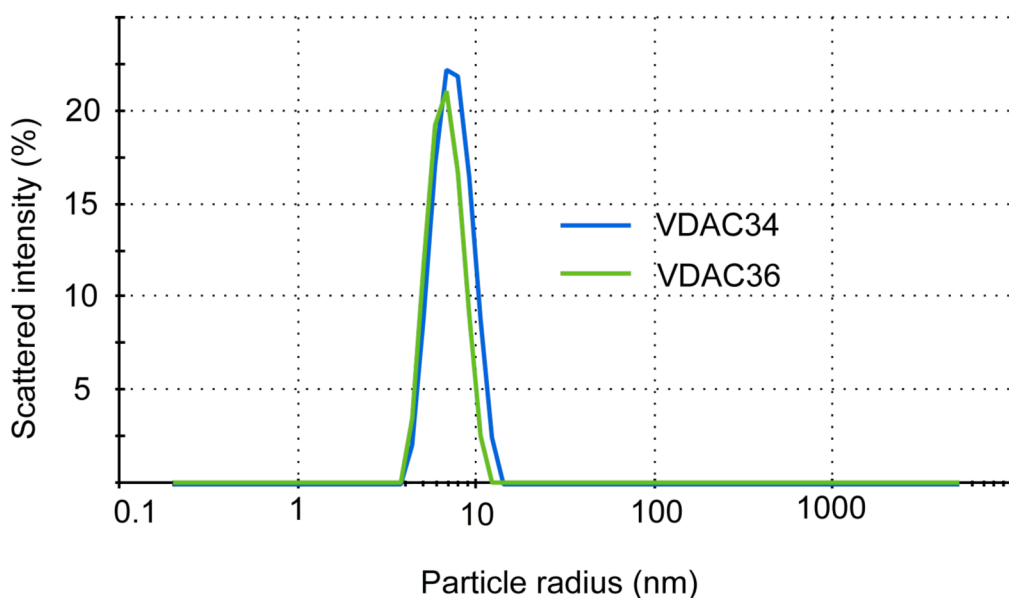


Figure S2. Analysis of stability and homogeneity of VDAC34 and VDAC36 by dynamic light scattering.

VDAC samples (at 14–17 μM) are soluble and stable in the presence of 1% (w/v) octyl- β -D-glucopyranoside. Size distributions derived from respective diffusion coefficients correspond to homogeneous populations of VDAC monomers in solution.

Supplemental Figure S3

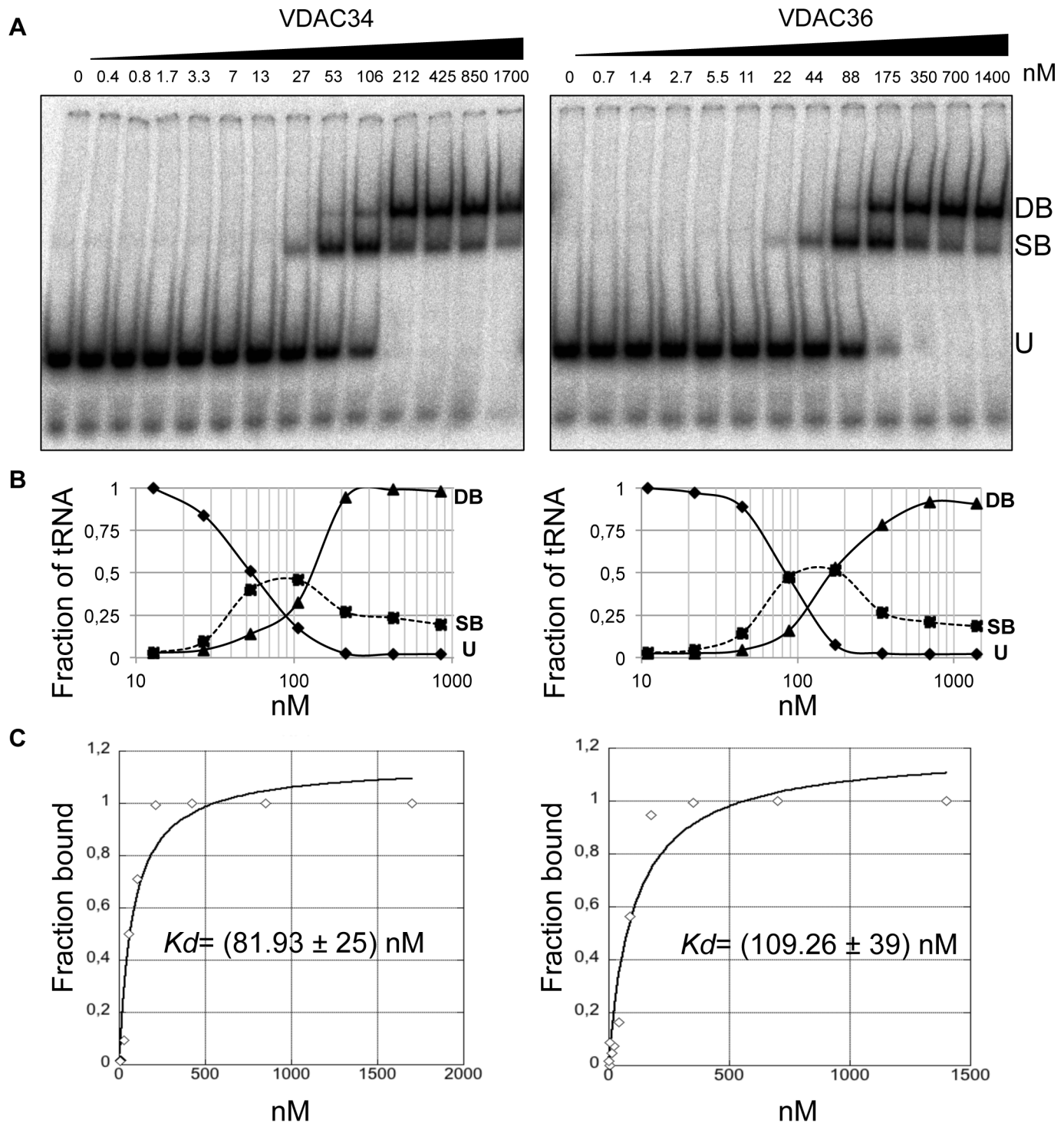


Figure S3. Affinity of VDAC34 and VDAC36 for tRNAs.

Example of gel-shift assays for quantitative analysis of tRNA-VDAC interaction in limiting tRNA conditions. (A) Gel-shift with 0.1 nM of tRNA and increasing amounts of VDAC protein. In gel-shift assays performed for quantitative analysis, 3 bands were visible and correspond to the unbound tRNA (U), the single-bound tRNA (SB) and the doubly-bound tRNA (DB). This indicate that the tRNA has 2 binding sites. (B) The curves for the 3 bands were plotted with protein concentrations on log scale. At $[\text{Protein}] = K_d$, the fraction of single-bound tRNA is 0.5 and the fraction of unbound and doubly-bound tRNA are 0.25 and this is what is expected for independent binding sites. (C) Graphics of binding curves. The apparent constant dissociation (K_d) values were calculated with KaleidaGraph 4.0 software.

Supplemental Figure S4

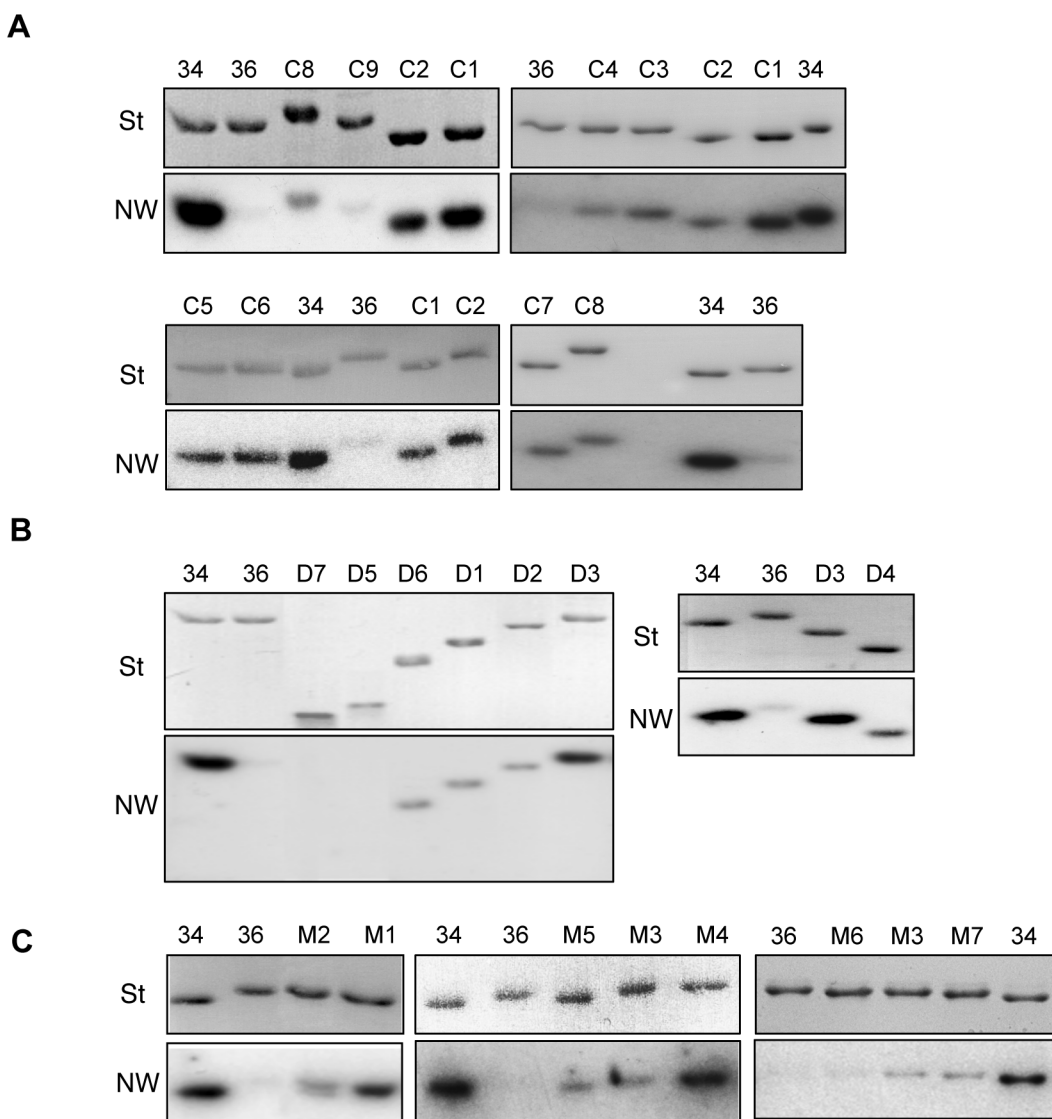


Figure S4. Northwestern analysis with mutant proteins.

Examples of Northwestern analysis with (A) chimeric mutants, (B) deletion mutants and (C) point mutants are given. (St) corresponds to the Coomassie blue staining of overexpressed proteins, fractionated on a SDS-PAGE and electroblotted on Immobilon-P membrane. (NW) corresponds to the Northwestern blot analysis. The proteins fixed on the membrane were renatured and incubated with radiolabeled cytosolic *A. thaliana* tRNA^{Ala} transcripts.

Supplemental Figure S5

BindN

VDAC34

Sequence:	MGKGPGLYTEIGKKARDLLYKDYQSDHKFSITTYSPTGVVITSSGSKKGDLFLADVNTQL
Prediction:	-----+-----+-----+-----+
Confidence:	550412401243717816522412132152421113135560090797336788683005
Sequence:	KNKNVTTDIKVDTNSNLFTTITVDEAAPGLKTILSFRVPDQRSGKLEVQYLHDYAGICTS
Prediction:	---+---+-----+---+-----+
Confidence:	007147235045121254329696675467014636052228019316339685877621
Sequence:	VGLTANPIVNFSGVVGTNIIALGTDVSFDKTGDFTKCNAGLSFTNADLVASLNLNNGD
Prediction:	-----
Confidence:	555173479594577624966862662432002031051326151496777272511033
Sequence:	NLTASYYHTVSPLTSTAVGAEVNHSFSTNENIITVGTQHRLDPLTSVKARINNFGKASAL
Prediction:	-----+-----+-----
Confidence:	040412222522721157344733342334367253123054351047386214407256
Sequence:	LQHEWRPKSLFTVSGEVDTKSVDKGAKFGGLALALKP*
Prediction:	-----+---+-----
Confidence:	8334405114417251420714183405667788155

VDAC36

Sequence:	MVKGPGLYSDIGKKARDLLYR DYVSDHKFTVTTYSTTGVAITASGLKKGELFLADVSTQL
Prediction:	-----+---+-----+-----+-----+-----
Confidence:	691523501232716815632737255262411111125371372500547789782074
Sequence:	KNKNITT DVKVTNSNVYTTITVDEPAPGLKTIFS FVVPDQKSGKVELQYLHEYAGINTS
Prediction:	-----+---+-----
Confidence:	000140235044110150328596655457028737995437018316339684767310
Sequence:	IGLTASPLVNFSGVAGNNNTVALGTDLSFDTATGNFTKCNA GLSFSSSDLIASLALNDKG D
Prediction:	-----
Confidence:	533261479484554432146742673642403041051324141224678277733033
Sequence:	TVSASYYHTVKPVNTAVGAELTHSFSSNENTLTIGTQHLLDPLTTVKARVNSYKGASAL
Prediction:	-----+-----+-----+-----+-----
Confidence:	047312121512623367465613242103115154346878881040293177274146
Sequence:	IQHEWRPKSLFTISGEVDTRAIEKSAKIGLAVALKP
Prediction:	-----+-----
Confidence:	833540512441735264074510250556677815

Figure S5. *In silico* analysis of VDAC34 protein with BindN software

The results obtained with BindN software correspond to the RNA binding prediction with a specificity equal to 95 %. Binding residues are labeled with (+) and in red. The non-binding residues are labeled with (-) and in green. The confidence is indicated from level 0 (lowest) to level 9 (highest).

Supplemental Figure S6

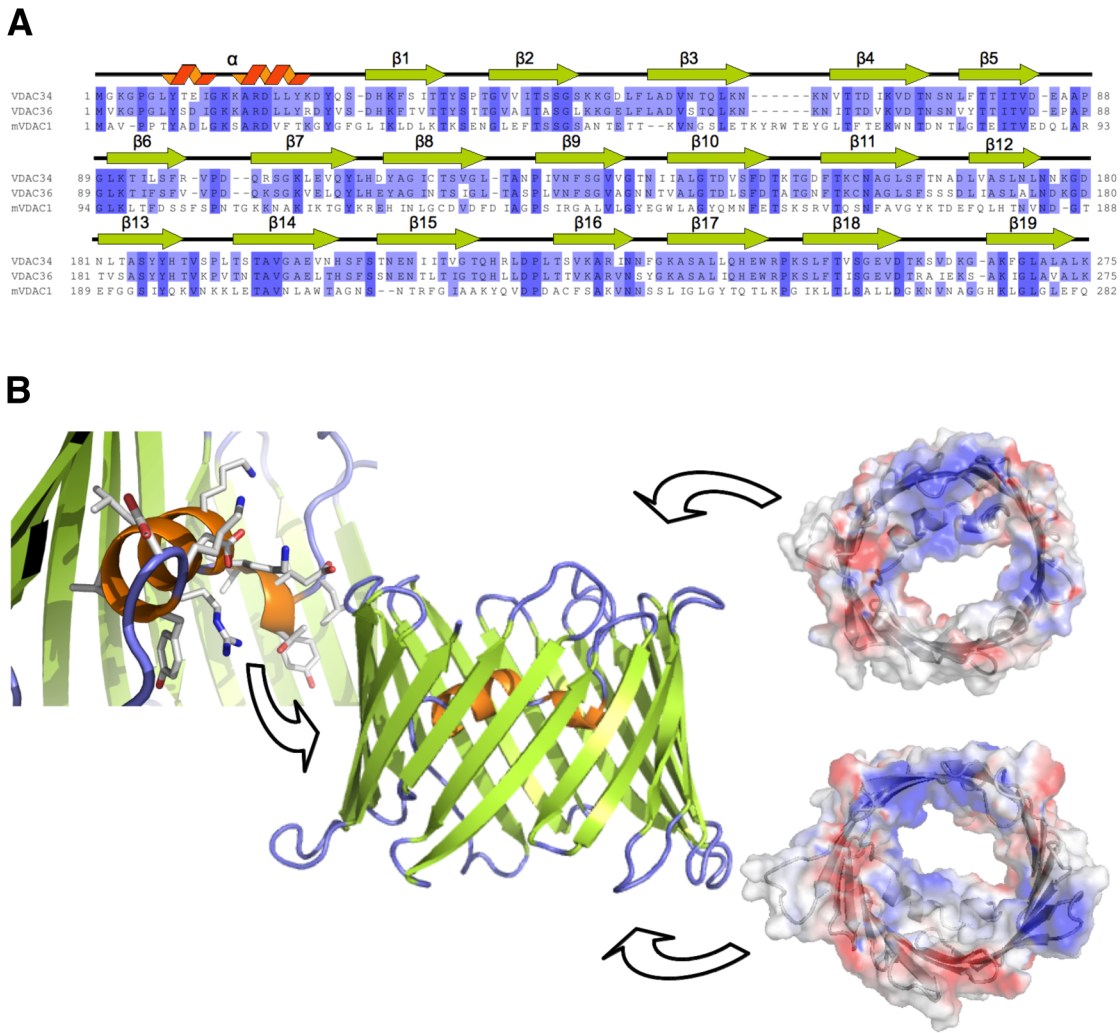


Figure S6. Structural features of *S. tuberosum* VDAC34.

(A) Sequence alignment of VDAC34 and VDAC36 with VDAC1 from mouse. Secondary structure elements are indicated above the sequences.

(B) 3D comparative model of VDAC34 based on mVDAC1 crystal structure depicted with the same color code (alpha helix in orange, beta-strands in green). On the left, a close up view on the amphiphilic helix making hydrophobic contacts to the channel's wall and pointing polar and charged groups inside the pore. On the right, electrostatic surface potential of channel entries shows high density of electropositive patches inside the channel. Blue indicates positive charges whereas red shows negative charges.

Supplemental Figure S7

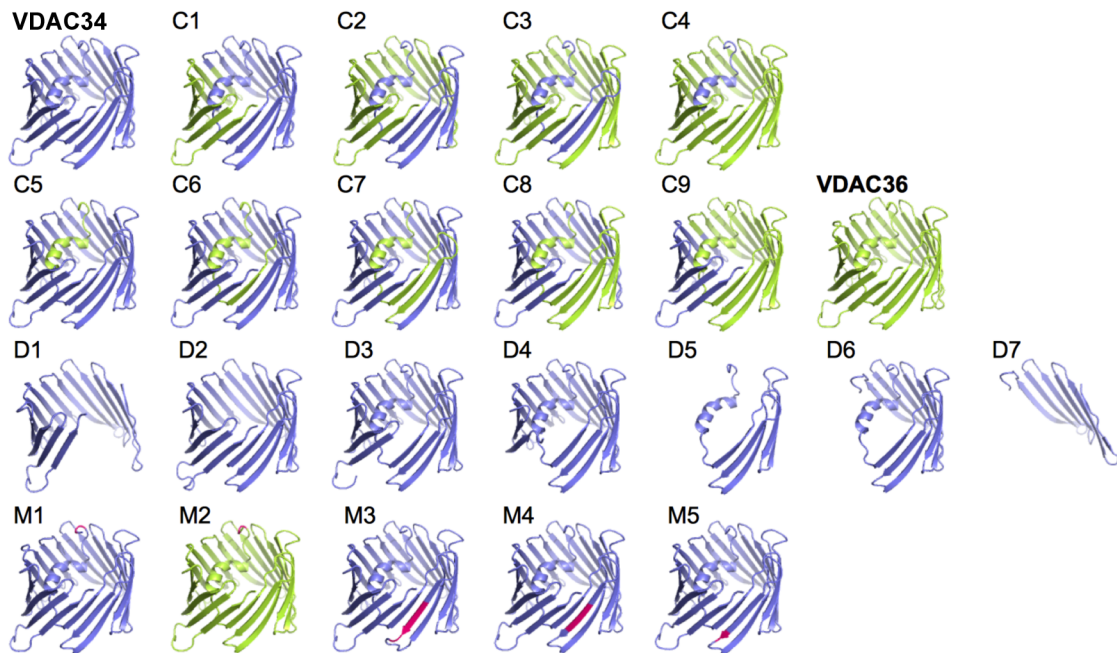


Figure S7. Collection of VDACs and mutants.

The models of VDAC34 and VDAC36 are depicted in blue and green, respectively. The C series corresponds to chimeric mutants and the same color code is used to indicate the origin of sequence segments. The D series corresponds to deletion mutants of VDAC34 and M1-5 represent point mutants of VDAC34 or VDAC36 with mutated positions highlighted in red.